IMPROVING WITH PROBABILISTIC AND SCALE FEATURES THE BASQUIN LINEAR AND BI-LINEAR FATIGUE MODELS

H. Usabiaga[1*], M. Muniz-Calvente[2], M. Ramalle[1], I. Urresti[1], A. Fernández Canteli[2],

[1]Ikerlan Technology Research Centre, Basque Research and Technology Alliance (BRTA), Jose Maria Arizmendiarreta pasealekua, 2. 20500 Mondragon, Spain

[2]Dep. of Construction and Manufacturing Engineering, University of Oviedo, Campus de Viesques 33203 Gijón, Spain

ABSTRACT

Although mechanical fatigue is considered stochastic in nature and there is a trend in industry towards reliability-based design, most popular high cycle stress-based fatigue models applied by industry still relies on deterministic methods. This is evidenced by the absence of integral probabilistic approach for predicting local and global probabilities of failure of structures in fatigue analysis commercial codes. In this paper, a probabilistic extension of the classical Basquin linear and bi-linear fatigue models, which are the most commonly promote by standards (ASTM, UNE…) and Guidelines (FKM, DNV GL, VDI…), is proposed. The proposed models include the scale effect and the probabilistic character of the S-N field. This seems to be a judicious and recommendable option for the practicing engineer to face the real fatigue design of components under varying loading while ensuring safety enhancement. The proposed enhanced model is implemented into the NCode2020 software to illustrate the possible implementation in general commercial codes focused on fatigue design. Finally, the applicability of the procedure proposed is illustrated by means of a practical example that includes the evaluation of experimental results and the prediction of failure for an Open-Hole-Plate.

Keywords: Probability; Fatigue; Linear and Bi-Linear Model, p-S-N fiel, probabilistic Miner rule

Nomenclature

A	Slope of Basquin model
A_i	i^{th} slope of bi-linear curve
B	Vertical axis intersection of Basquin model.
B_i	i^{th} vertical axis intersection of bi-linear model.
B_D	Damage variable of the Basquin and bi-linear models
GLM	Generalized local model
GP	Generalized parameter (driving force)
M	Miner number
N	Number of cycles
$\overline{N}$	Number of cycles corresponding to load steps of Miner rule
$N^{`}$	Equivalent number of cycles
CDF	Cumulative distribution function
P_{fail}	Probability of failure
P_{global}	Global probability of failure
S_{new}	Specimen/finite element size
$S_{original}$	Original size of the specimens tested in the experimental program
S_i	i^{th} subdomain of S-N in bi-Linear model
λ	Weibull location parameter
β	Weibull shape parameter
δ	Weibull size parameter
Δσ	Stress range

* Corresponding author:
E-mail address: husabiaga@ikerlan.es

1. Introduction

Components and structures subject to variable loading over time might lead to premature failures due to fatigue damage [1,2]. Moreover, the stress state associated with the fatigue failure remains far below the static material strength, which often leads to unexpected failures. For that reason, developing methodologies for accurate estimation of the fatigue strength of materials is crucial in order to ensure safe design and maintenance of structures and components.

Fatigue models are mainly focused on predicting the service life (N) of components in terms of a particular generalized parameter (GP) defined by the failure criterion selected, such as equivalent range of stresses or strains, Smith–Watson–Topper parameter [3], Fatemi-Socie parameter [4], among others [5]. This relation GP-N is determined experimentally by performing tests at different GP values and registering the number of cycles until failure. Despite the large scatter associated with those experimental results, the vast majority of models devoted to fit the GP-N field are purely deterministic.

The two models most used to fit the GP-N field in research and industry environments are the Basquin linear model [6], and the bi-linear model. Some examples confirming this affirmation could be the ASTM E739-10 standard [7] and VDI 2230 guideline [8], that considers the use of Basquin approach; and the EN1993-1-9 (Eurocode 3) standard [9], FKM [10], IIW [11] and DNVGL [12,13] guidelines prone to use the Bi-linear approach. This situation leads researchers and design engineers to develop and apply new alternative models to predict the service life (N) of components subject to a certain load history (referred to a driving force here denoted generalized parameter GP) to overcome the deterministic point of view implied by those standards or guidelines which promote the lack of probabilistic information, particularly, in the previous fatigue characterization phase.

According to a recent article [14] that reviews the state of the art about probabilistic S-N fields defined by statistical distributions, fatigue life prediction is feasible to be performed by deterministic models implying only mean or median S-N curve estimations, but the availability of reliable P-S-N fields of materials is crucial in the design of real components to take into account the influence of fatigue life scatter. During the last decades, some authors have introduced different probabilistic models, such as the Weibull Fatigue regression model proposed by Castillo and Canteli [15], or the probabilistic model proposed by V.V. Bolotin [15, 16] or A.M. Freudenthal [17, 18], among others [19–23]. Although these probabilistic models present a clear advance in the evaluation of experimental fatigue results, researchers and engineers are still reluctant to apply them to the practical design, possibly because the supposedly complicated implementation compared to that implied in the deterministic approaches. For this reason, in this work, a comprehensible probabilistic extension of the simplest deterministic, and most used models, i.e. the linear and bi-linear ones, to characterize the GP-N field are presented, in order to promote a probabilistic practical design of structures and components based on more safe and reliable structural integrity principles, which include the size effect as a natural, concomitant improvement of those models.

With this aim, a model is to carry out probabilistic predictions taking into account the scale effect is introduced. A new way of assessing fatigue damage accumulation in a probabilistic way is also presented. The probabilistic method proposed is applied to the characterization of a 42CrMo4 steel [25] and, subsequently, to the probabilistic failure prediction of a real component.

This paper is organized as follows: Firstly, the probabilistic approach applied to the linear and bi-linear models is presented. Following, the procedure is introduced to take into account the scale effect and the damage accumulation in a probabilistic way. Thereafter, the applicability of the procedure proposed is illustrated by means of a practical example. Finally, the models and results are discussed, and the main conclusions of the paper summarized.

2. Probabilistic fatigue characterization models

In this section, two probabilistic models to characterize the fatigue crack initiation have been developed and implemented based on the Basquin Model, which establish a linear relation between GP and N in a log-log scale.

2.1. Linear fatigue-life probabilistic model

The linear fatigue life probabilistic approach presented in this section is based on the well-known Basquin model, which is defined as:

$$\log(GP) = A \cdot \log(N) + B \tag{1}$$

where N is the number of cycles until fatigue failure, GP is the generalized parameter defined by the failure criterion selected ($\Delta\sigma, \Delta\varepsilon, SWT$ …), and, finally, A and B are the slope and the vertical intercept of the line defined by the model. Assuming that the distribution of the probability of failure does not depend on the GP level in a logarithmic scale (See Fig. 1), the percentiles lines are parallel to each other at log-log scale, so that the Basquin damage (B_D) representing the distribution of the fatigue failure can be defined as:

$$B_D = \log(GP) - A \cdot \log(N) \tag{2}$$

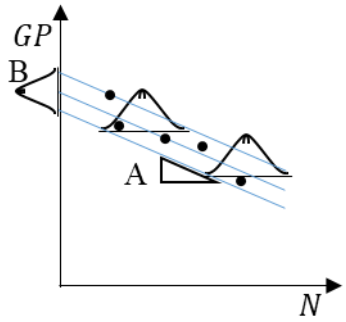

***Figure 1**. Illustration of the linear fatigue-life probabilistic model proposed*

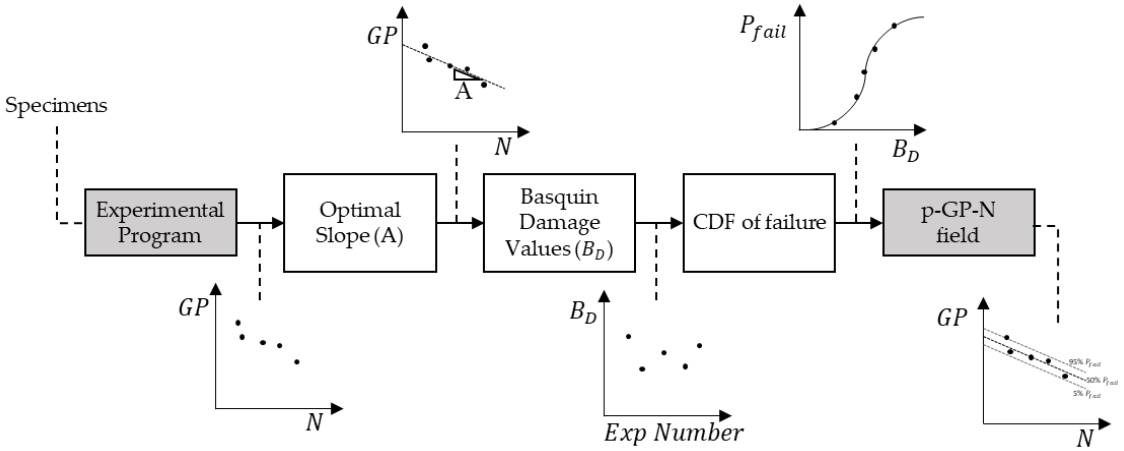

***Figure 2**. Flowchart of the Linear fatigue-life probabilistic model*

The definition of B_D allows us to develop a new approach to characterize the probabilistic fatigue field (p-GP-N) based on experimental results associated with different load levels. This approach is illustrated in figure 2, and the main steps are briefly described below.

Step 1: Experimental program (GP, N)

Obviously, the first step in a material characterization process consists in performing the experimental program in order to get data related to the phenomenon under study. In this case, the fatigue tests are usually performed under constant amplitude loading, which implies constant amplitude of remote stresses ($GP = \Delta\sigma$), representing the parameter most commonly associated with fatigue failure. Nevertheless, this model could be used for any other type of fatigue parameter (e.g. $GP = \Delta\varepsilon$), which varies according to type of test performed to guarantee constancy of those values during the experimental test (e.g. stress or displacement amplitude, SWT parameter, etc.). The results of this step are represented as different points on the GP-N field (See Fig. 2).

Step 2: Optimal Slope (A)

The Basquin model assumes linear relation between GP and N on a logarithmic scale (See Eq.(1)), so that the best slope (A) associated to this relation can be obtained by the linear least squares method:

$$A = \frac{n\sum_{i=1}^{n}(\log(GP_i)\cdot\log(N_i)) - \sum_{i=1}^{n}(\log(GP_i))\cdot\sum_{i=1}^{n}(\log(N_i))}{n\sum_{i=1}^{n}(\log(N_i)^2) - (\sum_{i=1}^{n}\log(N_i))^2} \quad (3)$$

where *n* is the number experiments performed.

Step 3: Basquin Damage Values (B_D)

Once the slope of the line is obtained, the value of the Basquin damage associated with each experimental failure is calculated, as the combination of the value of the GP imposed and the number of cycles until failure, given by Eq.(2).

The Basquin damage associated with each specimen failure is interpreted as the translation to the vertical axis of each point in a parallel way to the optimal slope obtained at the previous step (See Fig. 3).

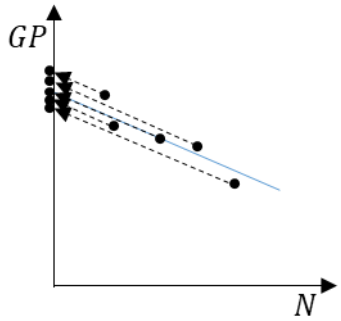

***Figure 3**. Illustration of the interpretation of the Basquin fatigue Damage*

Step 4: Cumulative distribution function (cdf) of failure

At this step, a probability of failure will be assigned to each B_D value obtained in the previous step and the cumulative distribution function (cdf) will be fitted. To do it, all B_D values are sorted in ascending order and after using a median rank estimator [26,27] the probability of failure of each of them is established:

$$P_{fail_i} = \frac{i - 0.3}{n + 0.4} \quad (4)$$

where *i* corresponds to the number associated with each experiment after being sorted in ascending order according to the B_D values, and n is the total number of experiments.

After that, the results are fitted to a three-parametric Weibull cdf [28],

$$P_{fail} = 1 - exp\left\{-\left(\frac{B_D - \lambda}{\delta}\right)^{\beta}\right\}; B_D > \lambda \tag{5}$$

where λ, β and δ are the location, shape and scale Weibull parameters respectively. This fitting process is easily performed using the maximum likelihood method or the Weibull probabilistic paper.

Step 5: Definition of the p-GP-N field

Finally, the *GP-N* lines identified as iso-probability failure lines are obtained by combining Eq. (2) and Eq.(5):

$$\log(GP) = A \cdot \log(N) + \left\{[-\log(1-P)]^{\frac{1}{\beta}} \cdot \delta + \lambda\right\} \tag{6}$$

thus, providing the $p\text{-}GP\text{-}N$ field shown at the final step of Fig.2.

Notice that this methodology allows us to perform the joint evaluation of all experimental results associated with different GP values, so that replicating tests at the same GP level [29], as customarily performed in current fatigue programs the last decades, may be avoided without any influence on the data assessment. In fact, it implies potentially either reduction of costs associated to the experimental fatigue campaign, because less number of specimens needs to be tested, or reliability enhancement of the data assessment, as a result of the advantageous test planning implied by more free and possible uniform choice of the *GP* in the experimental program.

2.2. Bi-linear fatigue-life probabilistic model

As in the previous model, the Bi-linear Basquin damage (B_D) is defined in this case allowing us to develop a new approach to characterize the probabilistic fatigue field ($p\text{-}GP - N$). This approach is illustrated on figure 4, which comprises the main steps as briefly described below.

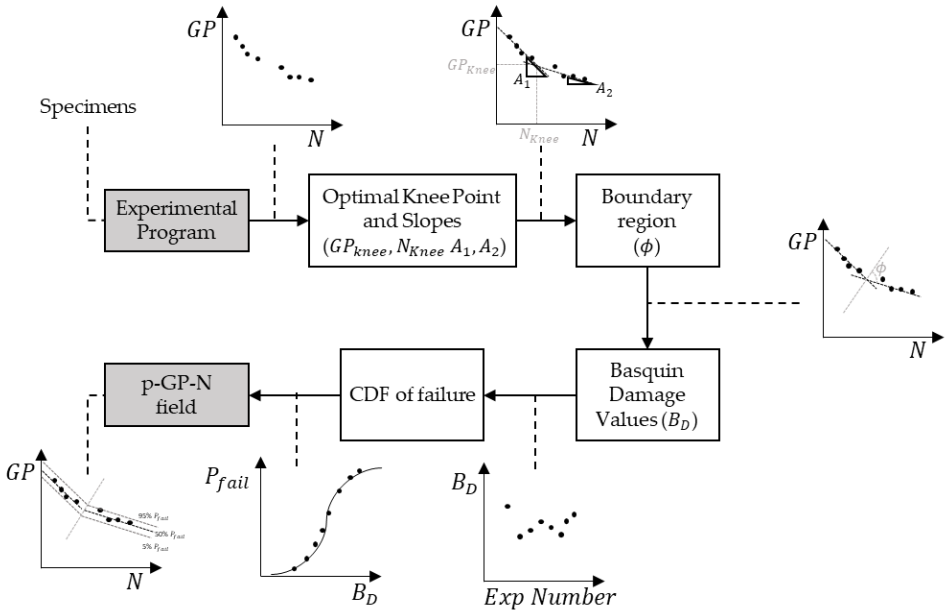

***Figure 4**. flowchart of the Bi-Linear fatigue-life probabilistic model proposed*

Step 2: Optimal slope (A_1 and A_2) and knee-Point (GP_{Knee}, N_{Knee})

In order to obtain the knee-point and optimal slope of the lines associated to each fatigue region, two data sets are created.

To do it, the failures are sorted in ascending order of the number of cycles to failure (N) obtained experimentally and the sets are defined as follows:

$$first\ set \rightarrow experiments \in [1:m] \qquad (7)$$
$$second\ set \rightarrow experiments \in [m+1:n]$$
$$m \in (1,n)$$

where m is an intermediate point and n is the total number of test performed. Initially, the number of experiments associated with each set is unknown, so that the *n-2* different possible *m* values are considered. After that, the optimal slopes (A_1, A_2) (Eq. (8)) and intersections (B_1, B_2) (Eq. (9)) with the vertical axis for each set are obtained for each m value by applying the least squared method.

$$A_1 = \frac{m\sum_{i=1}^{m}(\log(GP_i)\cdot\log(N_i)) - \sum_{i=1}^{m}(\log(GP_i))\cdot\sum_{i=1}^{m}(\log(N_i))}{m\sum_{i=1}^{m}(\log(N_i)^2) - (\sum_{i=1}^{m}\log(N_i))^2} \qquad (8)$$
$$A_2 = \frac{(n-m)\sum_{i=m+1}^{n}(\log(GP_i)\cdot\log(N_i)) - \sum_{i=m+1}^{n}(\log(GP_i))\cdot\sum_{i=m+1}^{n}(\log(N_i))}{(n-m)\sum_{i=m+1}^{n}(\log(N_i)^2) - (\sum_{i=m+1}^{n}\log(N_i))^2}$$

$$B_1 = \frac{\sum_{i=1}^{m}\log(GP_i) - A_1\sum_{i=1}^{m}\log(N_i)}{m} \qquad (9)$$
$$B_2 = \frac{\sum_{i=m+1}^{n}\log(GP_i) - A_2\sum_{i=m+1}^{n}\log(N_i)}{n-m}$$

Finally, the R-Squared index of each pair of sets is calculated and the sum of both R-Squared index pair is identify as the reference parameter to determine what is the optimal *m* value (the highest the R-Squared value, the better the solution). The knee point is then calculated by finding the intersection between the optimal pair of lines:

$$\log(N_{knee}) = -\frac{B_1 - B_2}{A_1 - A_2} \qquad (10)$$
$$GP_{knee} = A_1\cdot\log(N_{knee}) + B_1$$

Step 3: Boundary between the two regions.

The S-N domain is divided in two subdomains (S_1 and S_2). The leftmost domain, related to lowest cycles, will be linked to the A_1 slope, whereas the rightmost domain, related to highest cycles, will be linked to A_2 slope. A log-log straight boundary is proposed to define the boundary between both subdomains. In this work, the boundary between both regions is automatically determined without user's intervention. This boundary must ensure the compatibility between the failure probability for both domains. In other words, the cumulative distribution function associated with the Basquin failure hazard in both domains should be as similar as possible on the boundary region (See Fig. 5).

Once the boundary region is defined, the calculation of fatigue damage will be different according to the position of each experiment. On the one hand, the Basquin damage associated to the experimental results located at the left part of the boundary limit is calculated as in the linear model, by transferring the results directly to the vertical axis (*GP*) by Eq.(2) (See Fig (3)). On the other hand, the experimental results linked to the S_2 domain are transferred to the boundary between both domains and, after that, to the vertical axis according to Eq. (2).

To define the linear log-log boundary (See Fig. 5) between both domains the following algorithm is used:

a. Boundary line is defined by a point and slope. The point is defined as the intersection between the two optimal log-log lines defined at step 2 of this section. All knee point candidates for boundary slope are considered from the open interval defined by the A_1 and A_2 slopes, $\mathrm{A_b} \in (-\infty, \mathrm{A_1}) \cup (\mathrm{A_2}, +\infty)$.
b. B_D corresponding to every pair of GP-N is calculated and classified according to their domain (S_1 *or* S_2).
c. The P-value of k-sample Anderson-Darling test [30] related to sets of domains S_1 and S_2 is calculated in order to measure their similitude.
d. Proceed with the next slope candidate.

Steps b-d are repeated until the n_c candidates of boundary slope are considered. The one with the highest p-value is finally selected.

Once the slopes and the boundary line are defined, the B_d sets of the optimal slope are merged into a single set. The result of this step is the damage (B_D) associated to each experiment, that is given as a combination of number of cycles (N) until failure and the GP value.

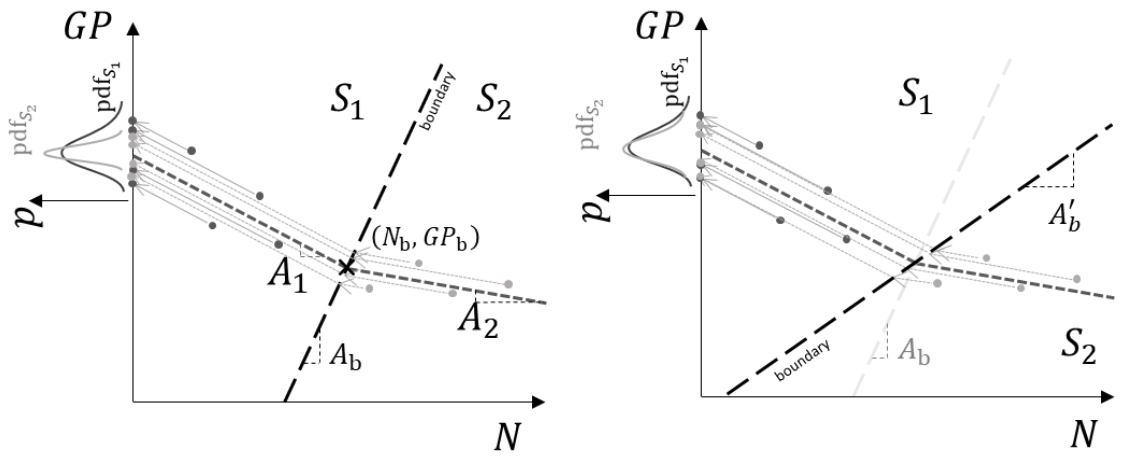

(a) (b)

Figure5*. (a) Schematic illustration of a non-optimal slope obtained during optimization process, and the pdfs associated to each domain;(b) Schematic Illustration of an optimal solution, and pdfs reached for the Bi-Linear Probabilistic fatigue Model*

Step 4: Cumulative distribution function (CDF) of failure

As in the linear probabilistic model, a probability of failure is assigned to each B_D value obtained in the previous step (See Eq(4)) and a Weibull cdf is fitted (See Eq (5)). The procedure in the Bi-linear case is the same as in the linear case.

Step 5: Definition of the p-GP-N field

Finally, the p-GP-N field is defined in two parts divided by the boundary line defined in step 3:

$$\log(GP) = A_1 \cdot \log(N) + \left\{[-log(1-P)]^{\frac{1}{\beta}} \cdot \delta + \lambda\right\}; Left\ part\ of\ p-GP-N \quad (11)$$

$$\log(GP) = A_2 \cdot \log(N) + \left\{[-log(1-P)]^{\frac{1}{\beta}} \cdot \delta + \lambda\right\}; Rigth\ part\ of\ p-GP-N$$

It is important to mention that this Bi-linear model allows all experimental results in the same cdf to be taken into account, independently of the *GP* value associated to each of them or their position in the p-GP-N field (left or right part). This is a consequence of the continuity between the two regions on the boundary limit, which is a condition the model must necessarily fulfil.

3. Probabilistic prediction of fatigue failure

According to the models described above, the probability of failure associated to any pair of GP and N can be easily obtained. Nevertheless, further advantages in the classical linear and bi-linear models could be achieved by incorporating the scale effect [28–30] and a probabilistic cumulative damage concept in the damage analysis of fatigue under variable loading even based on the classical deterministic Miner rule[34]. Both implements are already included in some regression Weibull models [15] representing a notably advance in the component design. In fact, they are indispensable tools for guaranteeing transferability of the experimental results from the laboratory tests to the practical component design contributing to more reliable fatigue failure predictions

3.1. Scale and stress concentration effects

It is well known that the fatigue failure is influenced by the scale effect [28,29] though usually it is disregarded by classical deterministic fatigue models. This may be assigned to the lack of an analytical equation to perform the transformation from one scale to another. On the contrary, the probabilistic fatigue models introduced in this paper imply the scale effect in their definition according to the Weibull cdf expression:

$$P_{fail} = 1 - exp\left\{-\frac{S_{new}}{S_{ref}}\left(\frac{B_D - \lambda}{\delta}\right)^{\beta}\right\}; B_D > \lambda \quad (12)$$

where S_{ref} is the reference size of the experimental specimens used to obtain the p-GP-N field, and S_{new} is the size for which the probability of failure wants to be known. As can be seen, the p-GP-N field derived from the steps described in the previous sections is unequivocally associated with the size of the tested specimens through the scale parameter of the Weibull model (δ). Thus, the real fatigue lives of a

component should be in agreement with those predicted from the experimental results on specimens in the laboratory, while the use of Eq.(6) or Eq.(11) to predict the fatigue life of any other specimen or component, without any scale effect correction, is incorrect. For that reason, a correction of the GP distribution must be performed according to the scale effect:

$$\log(GP) = A \cdot \log(N) + \left\{ \left[-\frac{S_{ref}}{S_{new}} log(1-P) \right]^{\frac{1}{\beta}} \cdot \delta + \lambda \right\} \tag{13}$$

This modification makes it possible to carry out fatigue life predictions of larger components than those being tested in the laboratory (tests at reduced scale), which is the most obvious advantage, but it also allows further fatigue life predictions to be performed based on GP distributions obtained from finite element (FEM) calculations. Taking into account the local GP values at each finite element for a given mesh, the element size (S), and the number of cycles (N), it is possible to assess the probability of fatigue failure of any finite element using Eq. (13). The graphical representation of the local probability of failure for the finite element mesh is known as hazard map [35], which provides to the design engineer a practical valuable information to check or improve the current design. Once the local probability of failure at each finite element is determined, the weakest link principle is applied to calculate the global probability of failure of the whole component using the expression:

$$P_{fail_{global}} = 1 - \prod_{j=1}^{ne} (1 - P_{fail_j}) = 1 - \prod_{j=1}^{ne} (exp\left\{ -\frac{S_{new_j}}{S_{ref}} \left(\frac{B_{D_j} - \lambda}{\delta} \right)^{\beta} \right\} \tag{14}$$

where *j* is the element under local study varying from 1 to the total number of elements (*ne*).

3.2. Damage accumulation

The most commonly used fatigue damage accumulation model is the Miner rule [34], which proposes damage being given as the relation between the number of cycles applied to the component ($\overline{N}_i$) at a certain GP level and the number of cycles associated with the expected fatigue life of the material (N_i) for that GP level:

$$M = \sum_{i=1}^{n} \frac{\overline{N}_i}{N_i} \tag{15}$$

As can be seen, according to the Miner rule, the total fatigue damage for a certain load history is calculated as the sum of the partial damages associated to each cycle (or block of cycles), $i \in [1, m]$. The classical Miner rule establishes deterministically that the component fails for M = 1.

On the other hand, the combination of the Miner rule with the models proposed in this paper enables the probabilistic interpretation of the Miner number to be accomplished. Since the Miner number represents the cumulative damage of the material fatigue strength, it follows that the fatigue strength of this material under varying load can be defined in a probabilistic way using the models proposed above. Thus, once the percentile (P) to which the critical number of cycles to failure N_i are referred to, is selected, the probabilistic proposal applied to the Miner rule establishes that failure occurs when M = 1 for the

probability of failure represented by that percentile. Consistent with this new approach, if the value of the Miner number is known for a given percentile after applying a load history, it would be possible to calculate the new Miner number associated with any other probability of failure, say between 0 and 0.99 and, inversely, to obtain for which probability of failure the result becomes.

Alternatively to the procedure described above, it is possible to apply a recursive process that accumulates probability of failure [15], [36] for the different loading blocks applied. Figure 6 shows a graphical explanation of the different steps implied in the accumulation of probability of failure as described below.

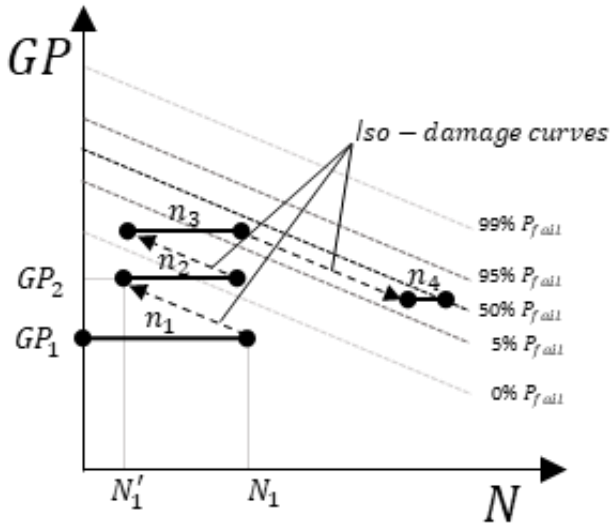

Fig. 6. Procedure for accumulating probability of failure

In Fig. 6 , the hypothetical first pair of GP and N applied are represented as $GP_1 - n_1$, and the damage associated to this loading block can be calculated by Eq.(16), B_{D1} . After that, a new loading block defined by $GP_2 - n_2$ is be added. To do that, it is necessary to transform the number of cycles associated to the previous blocks (N_1) to the equivalent number of cycles associated to GP_2 while maintaining the same probability of failure (N_1'), i.e. the same damage level, once the first step is concluded and before the second one is applied, which implies:

$$B_{D1} = B_{D1'} \rightarrow \log(GP_1) - A \cdot \log(N_1) = log(GP_2) - A \cdot \log(N_1') \quad (16)$$

Clearing N_1' in the previous equation, the equivalent number of cycles is given by:

$$N_1' = N_1 \left(\frac{GP_2}{GP_1}\right)^{\frac{1}{A}} \quad (17)$$

Finally, the accumulated damage after the second block (n_2) is calculated as:

$$B_{D2} = \log(GP_2) - A \cdot \log(N_1' + n_2) \quad (18)$$

This procedure is repeated as many times as loading blocks are defined in the loading history. In the illustrative example shown on Fig.6, the process is repeated four times and, at the end of each loading

block application, the fatigue damage obtained ($B_{Di}; i \in [1,4]$) is related to a probability of failure by Eq (14) ($P_{fail_i}; i \in [1,4]$). It is important to remark that the final probability of failure obtained from this procedure coincides with that calculated using the Miner rule following the procedure formerly described.

4. Model's implementation in a commercial software

Probabilistic damage approach reported in this analysis is implemented in a Hbm Prenscia NCode 2020 commercial code. The selection of this software is motivated on one hand by the dedicated fatigue analysis built-in routines and tools available in the code. Among other, this software includes routines for loading and processing multiple finite element code results, multiple stress combinations for generalized parameters, multiples mean stress corrections routines, time series generation, analysis, and processing routines, rainflow methods, post-processing libraries, etc. All these procedures make implementing a new fatigue approach in Ncode simpler than making it from scratch. On the other hand, Ncode is positioned as one of the standards durability analysis code in a broad range of industries. The customization capabilities of the software enable the implementation of new durability and fatigue approaches with almost the same functionality and interface than Ncode native fatigue and durability approaches. Accordingly, the learning curve of a skilled Ncode analyst for applying the new probabilistic approach is very low, making the dissemination and application of this new approach within industry easier.

4.1 Description of the implementation

The approach reported in this article is implemented by combining *Custom Analysis* glyphs and *Custom engine* using python v.3.6 programming language. Fig. 7 reports a schematic workflow of *Custom Analysis* Glyph.

The *Custom Analysis* glyph workflow retrieves the centroidal stress tensors, element by element, from the unitary load case solution. Then, it combines the stress tensor with its corresponding load time history. After that, within the *Custom Stress Combination* routine, the stress tensor is transformed into the GP, in this way converting a tensor time history into a scalar one. In this user case, maximum absolute principal stress is considered as GP. The GP time history is then processed by the Ncode built-in four-point rainflow algorithm, decomposing time history in multiple pairs of stress range and mean stress values. Each of GP pair computed by the rainflow is then passed to the custom engine together with the fatigue S-N material properties. The *Custom Engine* routine processes the input information and outputs accumulated elemental local probability according to the implemented Probabilistic Basquin and bi-linear approach. The *Custom Analysis* routine proceeds with all pairs of mean and range stress derived from the rainflow analysis (inner loop) and with all the finite elements of the model (outer loop) until local probability of failure is computed for all the elements in the considered domain. After that, the global probability of failure is estimated.

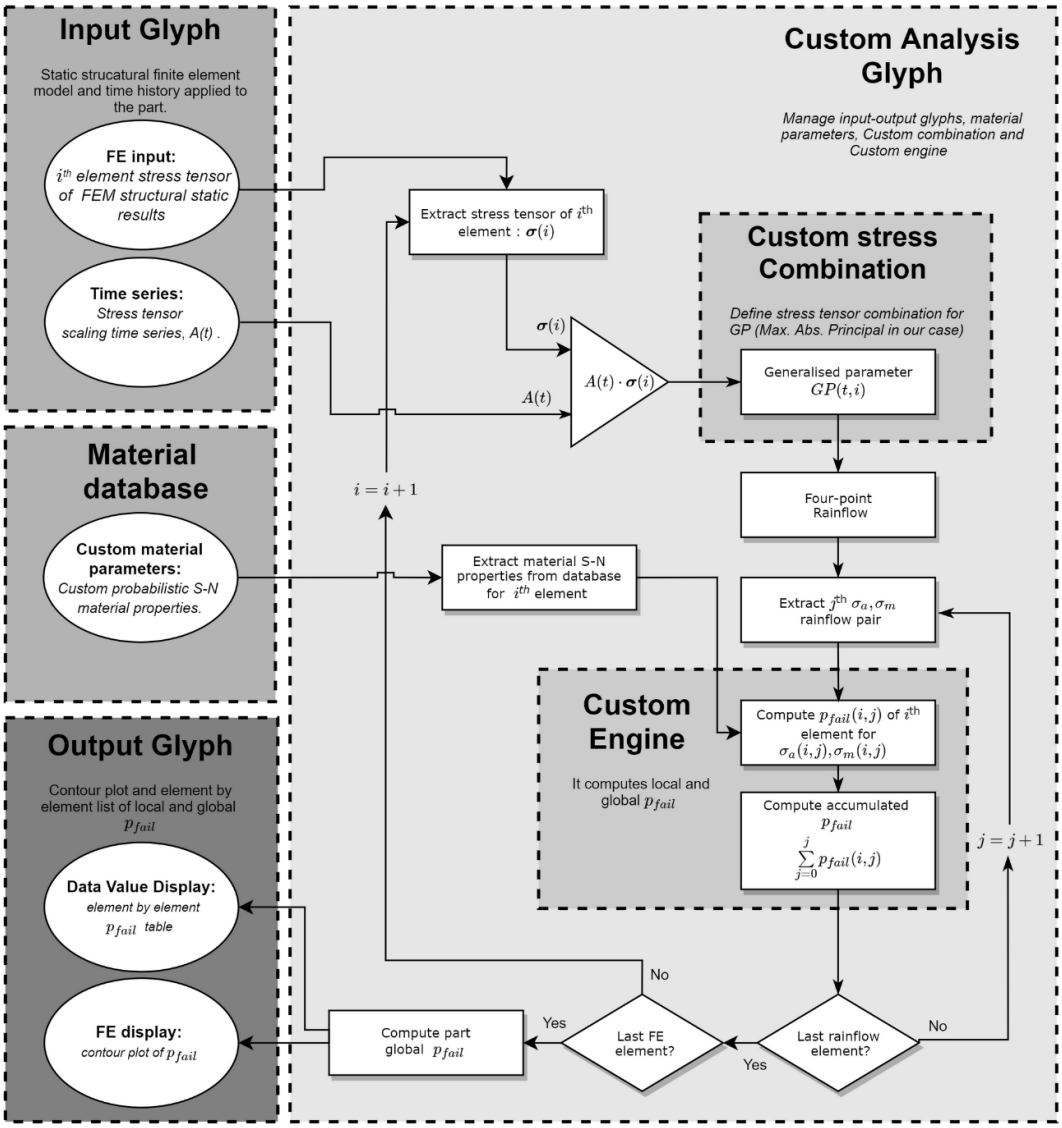

Fig. 7. NCODE workflow algorithm

The communication between *Custom Engine* and *Custom Analysis* is defined by four python functions to be programmed according to the applied probabilistic fatigue approach. Each of the routines has a particular purpose, namely:

- *Initialise():*defines and initializes the customized variables of the implemented probabilistic approach.
- *Reset():*is called by NCODE every time it a new element is considered. Exception is produced during the first element where Initialise function is called instead of Reset.
- *CalcCycleDamage():*deals with the core of the new probabilistic approach. It computes probability of failure of each element based upon the generalized parameter calculated by Ncode and the material properties related to the analyzed finite element.

- *GetCustomResults():* defines the output variable to be tabulated or graphically plotted in contours. In our case, this function basically defines element failure probability and global part failure probability. This function interface with

4.2. Environment for final users.

One of the main advantages of implementing the predictive models on a commercial software is the improvement on the widespread of the used of them, which will be accessible for fatigue expert users on a friendly environment. Fig. 8 depicts the interface of the implemented workflow in NCODE. The following list which includes the most important glyphs or modules:

- Input FE: includes the unit load finite element solution calculated by finite element software.
- Time history generator glyph: generates load time history.
- XY display glyph: plots a cycle of the applied dynamic loading.
- Custom Analysis: represents the main glyph of the approach model. (See Previous Section)
- Statistic glyph: computes the cumulative failure probability of the whole part.
- FE display glyph: plots contours of probability of failure for all the elements in the FEM.
- Data Value Display glyph: lists the accumulated probability of failure element by element.
- Multicolumn manipulation glyph: merges applied load amplitude and accumulated probability of failure of the part in a single variable.
- Data Value Display glyph (2): displays the applied force amplitude and corresponding accumulated probability of failure.

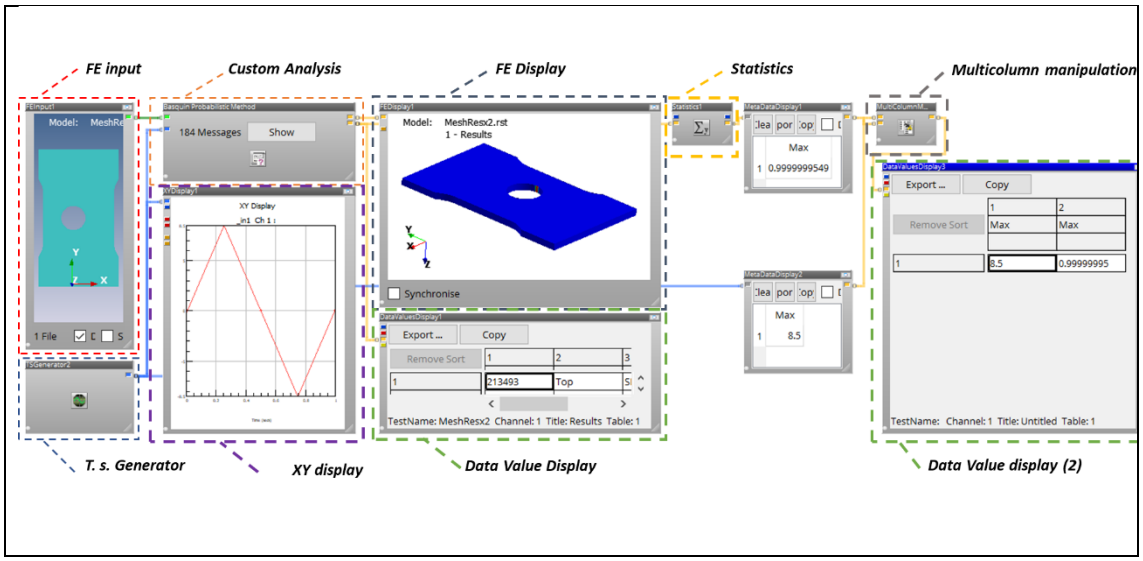

Fig. 8. Overview of the graphical NCODE workflow interface

5. Example of application

5. 1. Case study

To illustrate the applicability of the methodologies introduced in this paper, the experimental results from a fatigue characterization campaign on 42CrMo4 steel [25] (See Figure 9 and Table A1), are used to derive the probabilistic S-N field (p-S-N). Thereafter, the results are used to perform an example of prediction of failure of a component. This prediction also includes a study of the influence of the mesh size on the final fatigue failure prediction.

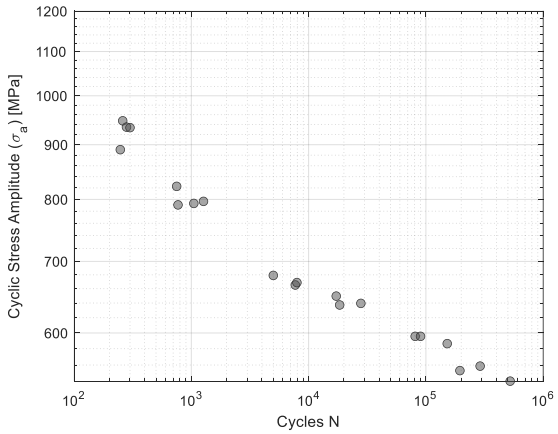

Fig. 9. Experimental results obtained during the fatigue characterization of the 42CrMo4 Steel [25]

According to the work of Boller and Seeger [25] the driving force associated with the fatigue failure of this material is the range of the maximum principal stresses. Accordingly, $\mathrm{GP} = \Delta\sigma_{\max}$ is adopted for the characterization and prediction phases of this case study.

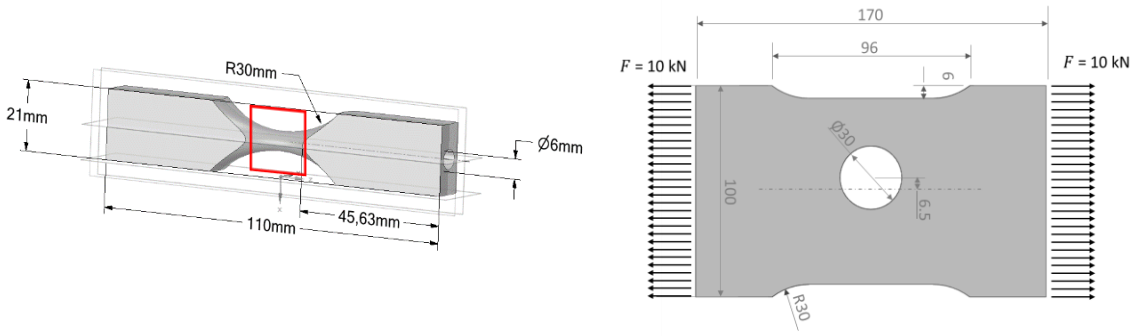

Figure 10. a) Geometry of the specimens used to perform the fatigue characterization and detail of the area considered as the reference size; b) Geometry of the specimens used for the illustration of prediction of probability of failure.

Once the p-S-N fields are calculated, they are used to obtain the probability of failure of a component subject to a local stress field completely different than the one present on the experimental characterization programme. Figure 10 shows the specimen geometry used to perform the fatigue characterization and to illustrate how the probability of failure is predicted. As could be expected, the stress field on the characterization specimen is almost uniform on its central part, and stress concentrations are avoided as much as possible. On the contrary, high stress concentration are common

in the design of components, usually originated by holes or notches, which differs from the load conditions applied on the laboratory during the characterization. To solve this problem, the methodology described in this paper enables the local distribution of the stress amplitudes in the fatigue problem to be take into account by converting it into a probability of failure contour plot and a global probability of failure. With the aim of demonstrating how these predictions are derived on a real case basis, a 6mm thick off-centred Open-Hole-Plate [37] (see Fig. 10) is used. The Open-Hole-Plate is subject to uniaxial cyclic constant amplitude loading at r =-1 ratio, when the relation between probability of failure and dynamic loading amplitude loading is obtained for three different number of cycles: 10^5, $5 \cdot 10^5$ and 10^6 cycles. About 100 simulations are carried out at monotonically increasing stress range for each approach and the three targeted number of cycles.

The following subsections describes the implementation and results of the fitting p-S-N field and the predictions of failure for the case under study.

5. 2. Fitting the p-S-N field for the proposed models

Following the methodologies described above, the GP-N experimental results (Fig.2) are fitted to a Basquin linear and bi-linear probabilistic models. In the case of the Basquin model, the first step consists in obtaining the optimal slope using the last squared method, which results $A_1 = -0{,}0728$. After that, the denominated Basquin damage (B_D), as defined in this work, is calculated for each pair of *GP-N* according to Eq (2). Following, the B_D are fitted to a Weibull CDF (See Figure 11(a)), which allows a relation between the probability of failure, the number of cycles and the values of the *GP* to be established (See Figure 11(b)). Note that this relation is associated with the size of the specimens tested in the laboratory (See Figure 10(a)). Considering that the most common cause of fatigue failure may be assigned to surface defects, the size to be considered is the surface of the specimens, instead of their volume. For the specimens tested in [25], the reference area is 419,4 mm^2.

On the other hand, the same fatigue data can be evaluated using the bi-linear probabilistic model. In this case, the first step consists in the calculation of the optimal knee-point ($GP_{Knee} = 693.69$ MPa; $N_{Knee} = 3872$) and the optimal slopes of both lines of the model ($A_1 = -0{,}1107$; $A_2 = -0{,}0504$). After that the angle defining the boundary limit between the two regions and the line defined by this angle and the knee-point ($\log GP = -5.5316\text{e}-4 \cdot \log N + 2.8432$) is defined. The next step consists in the calculation of the damage associated to each experiment at failure, so that all experimental points must be transferred to the vertical axis. To do that, the points on the right side of the field are transferred to the boundary line with a slope equal to A_2 and, thereafter, all experimental points are transferred to the vertical axis with the slope equal to A_1. Following, the B_D are fitted to a Weibull CDF (See Figure 11(c)) and the p-GP-N field is represented (See Figure 11(d)).

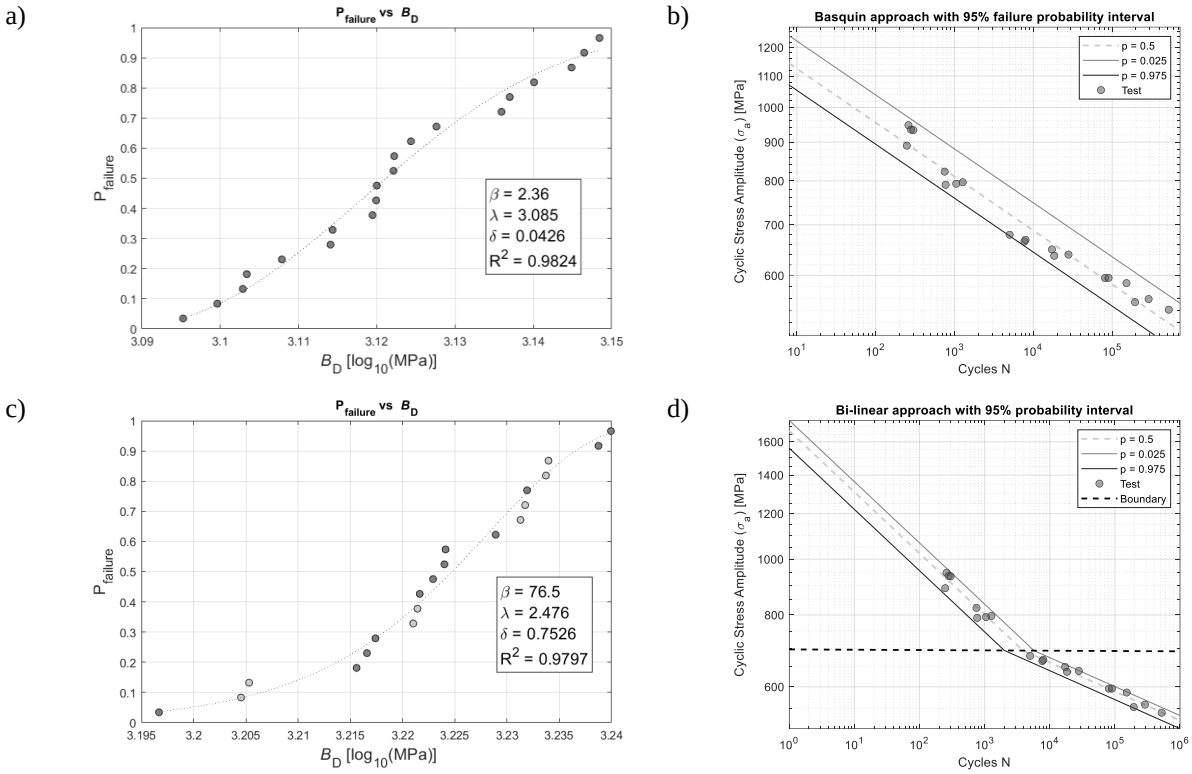

Fig. 11. Results for the linear(a,b) and bi-linear(c,d) probabilistic model: Estimated *Weibull cdf; (a,c) Resulting p-GP-N field, (b, d).* S_{ref}=419,4 mm^2.

5. 3. Failure prediction

The first step on the failure prediction for the components under study consists in the implementation of a finite element calculation in order to obtain the local stresses. To do that, Ansys Workbench Mechanical 2019 R3 software is used to derive the stress field for a reference tensile load (10 kN). Modelling assumes that load level is low enough to keep the material within the linear elastic range and under infinitesimal strains. Accordingly, a linear relationship between force and displacement is considered and any loading state of the Open-Hole-Plate subject to axial load is estimated from the solution of a single unitary loaded structural finite element model scaled by the corresponding applied load.

In order to check the suitability of the mesh size and its influence on the stress field and on the prediction of fatigue failure, three different mesh sizes are considered using hexahedral solid 186 three-dimensional iso-parametric quadratic elements. A reference mesh size is first defined, and in the other two mesh sizes the element edge length is reduced to the half of its predecessors. Figure 12 shows the considered three mesh types.

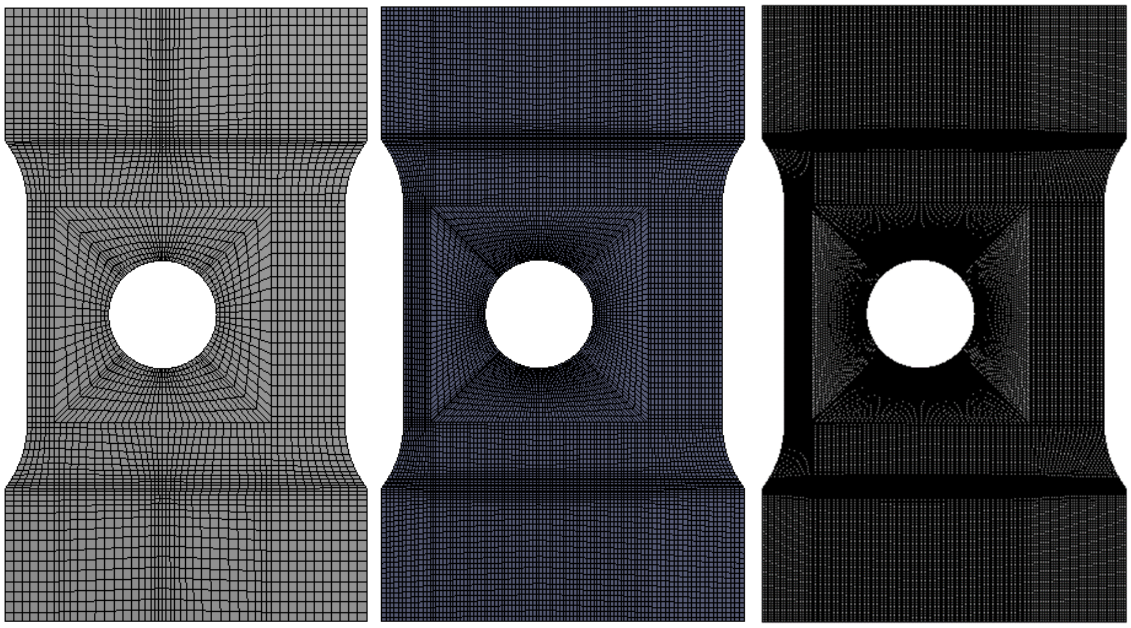

(a) (b) (c)

Fig. 12. Mesh discretization applied to the open hole: a) coarse; b) medium; c) fine

Figure 13 reports the maximum principal stress contour map of the unitary load case for the three mesh densities. Combining Richardson extrapolation and the grid convergence index the exact value of the maximum absolute principal stress in the most critical point of the coupon is estimated. The study reports an error on stresses estimation at the most critical point lower than 0.3% for all meshes, according to the Richardson Extrapolation. This means that all meshes can be used to estimate the real stress field across the component, so that any of them can be chosen to perform the fatigue analysis.

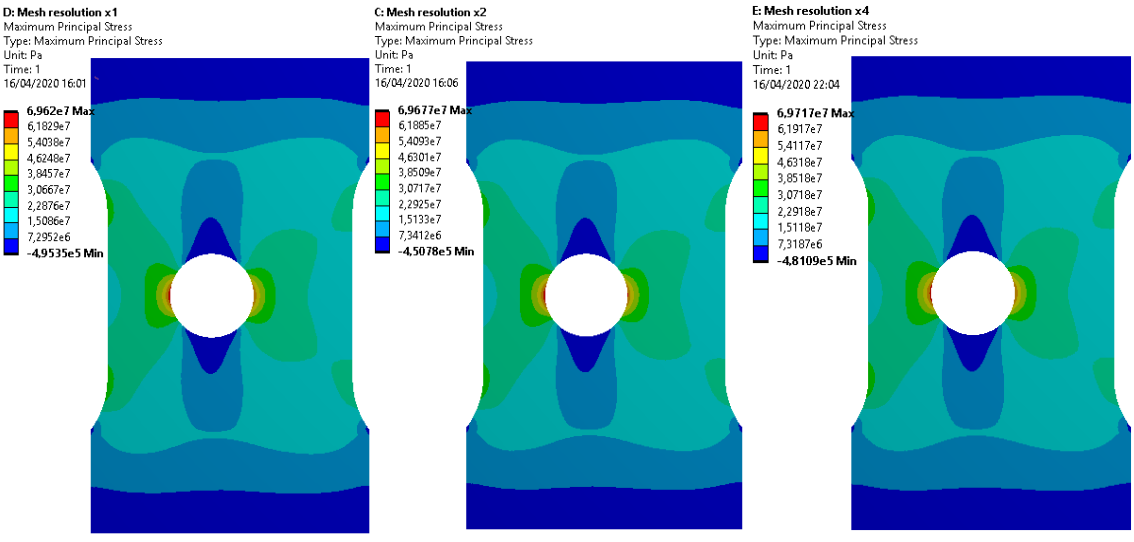

(a) (b) (c)

Fig. 13. Absolute principal stress at the open hole for the three mesh densities: a) coarse; b) medium; c) fine.

Once the maximum principal stresses are obtained using FEM, they are introduced into the custom probabilistic fatigue program implemented in NCode (See Section 4) in order to convert them into local failure probability contour plots. As an example, Figure 14 depicts the contour plot of local failure probability for $5 \cdot 10^5$ cycles for the Basquin linear (a-b) and bi-linear (c-d) probabilistic approaches, associated to a global probability of failure of 99%, which corresponds to an applied cyclic force amplitude of 85 kN and 115 kN for the Basquin linear (a-b) and bi-linear approaches, respectively.

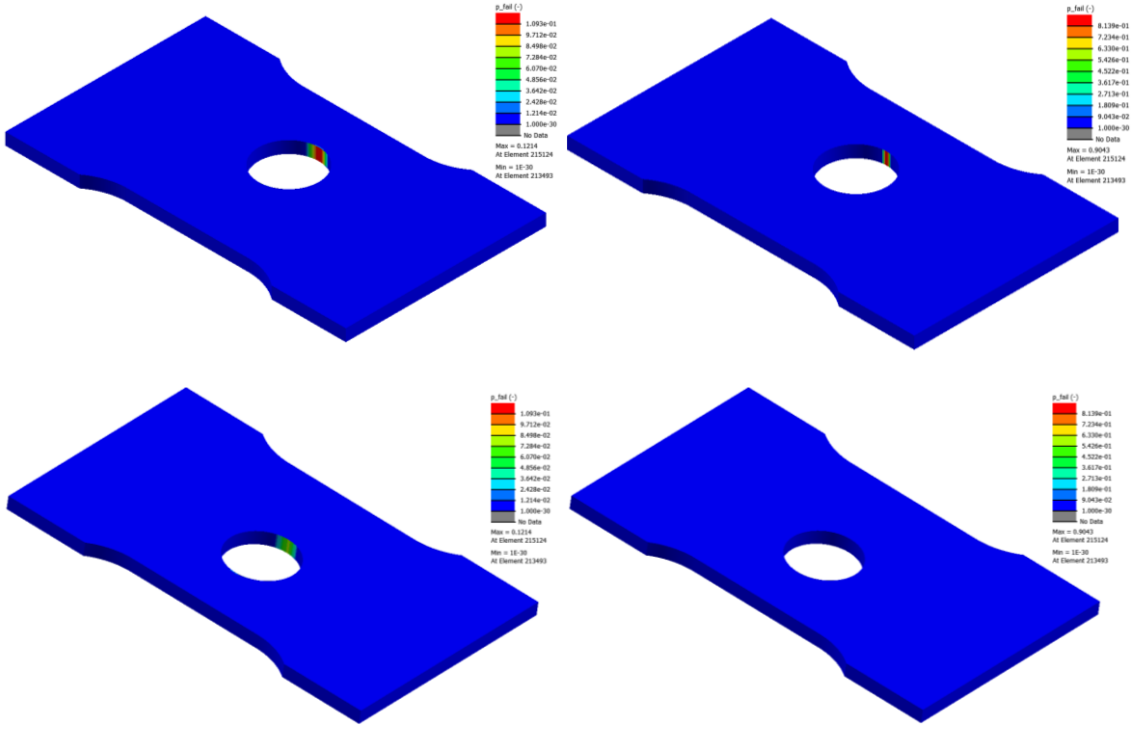

(a) (b)

Fig. 14. Contour plot of local probability of failure estimated by Basquin and Bi-linear approach: a) Basquin $F_a = 115\ kN$, $5 \cdot 10^5$ cycles (front and back face); b) Bi-linear $F_a = 85\ kN$, $5 \cdot 10^5$ cycles (front and back face).

Furthermore, the software enables the cumulative failure probability to be obtained in terms of the applied force amplitude. Figure 15 depicts an example of the relation between the dynamic loading amplitude and the probability of failure associated to the three targeted number of cycles (10^5, $5 \cdot 10^5$ and 10^6 $cycles$). Figure 15 also shows the influence of the discretization considered for the three mesh densities (all CDFs associated with each model are overlapping).

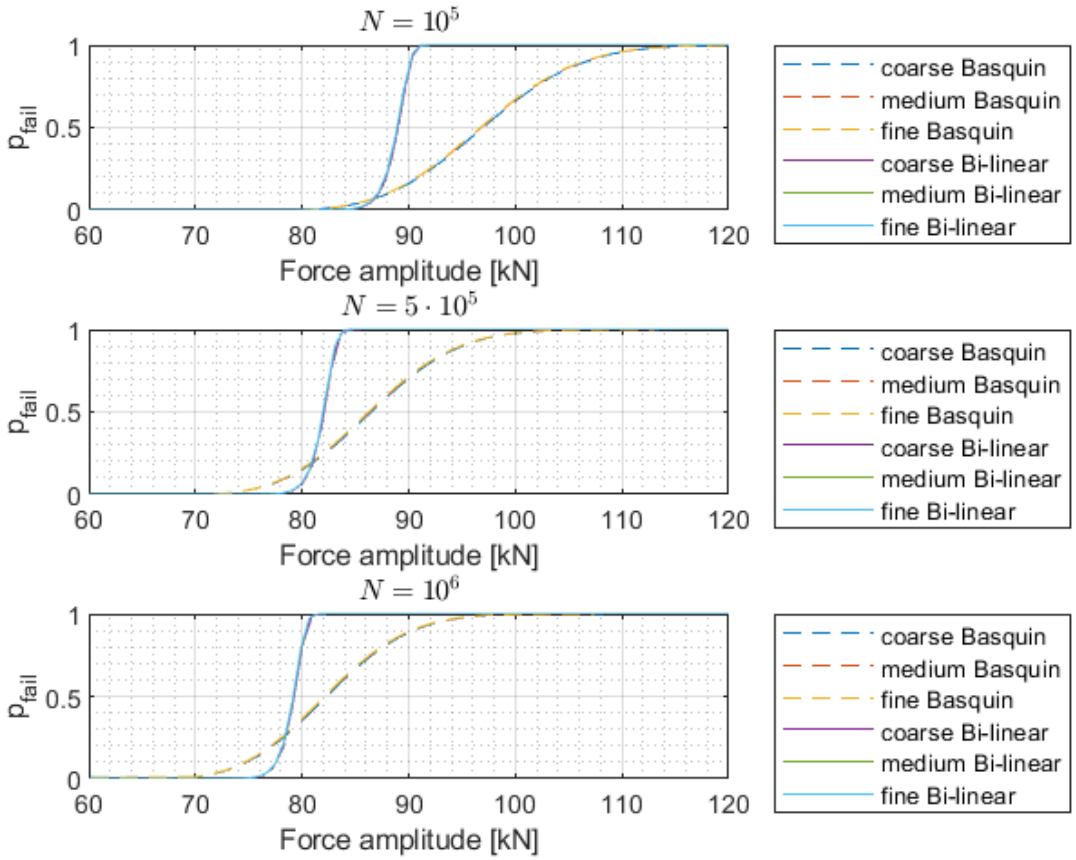

Fig. 15. Cumulative probability of failure vs force amplitude for the linear and bi-linear approach for 10^5, $5 \cdot 10^5$ and 10^6 cycles.

Finally, Table 1 shows the values of the force amplitude associated to different probabilities of failure for the target number of 10^5, $5 \cdot 10^5$ and 10^6 cycles. As can be seen, the relative error between both models, Basquin and Bi-linear, is lower than 9% in all cases.

Table. 1. Cyclic force amplitude prediction for $p_{fail} = 0.01$ 0.05 and 0.1

Cycles	*Value*	p_{fail} = *0.01*	p_{fail} = *0.05*	p_{fail} = *0.10*
10^5 cycles	*Basquin*	8.2217	8.5812	8.8098
	Double Basquin	8.5021	8.6475	8.7149
	Relative Error	-3.4%	-0.8%	1.1%
$5 \cdot 10^5$ cycles	*Basquin*	7.3314	7.6529	7.8549
	Double Basquin	7.8336	7.9694	8.0302
	Relative Error	-6.6%	-4.1%	-2.2%
10^6 cycles	*Basquin*	6.9788	7.2854	7.4774
	Double Basquin	7.5631	7.6948	7.7541
	Relative Error	-8.0%	-5.5%	-3.6%

6. Discussion

The paper presents two alternatives to fit a probabilistic fatigue field based on Basquin linear or bi-linear models. The main advantage of extending these models by a simple, but powerful, probabilistic approach is the general recognition that the Basquin model finds in the industrial environment. Almont all standards and guidelines are focused on the derivation and use of linear and bilinear fatigue models, so that practically all engineers related to reliability calculations are familiar with these models.

This paper would allow to introduce some probabilistic aspects related to the characterization of the fatigue experiments, and the used of p-S-N fields properly during the design of real components. Furthermore, the transferability of the scatter show during the characterization process can be easily transfer to the prediction of failure, which would lay the foundation for starting probabilistic fatigue life assessments in industry, where commercial software is generally used to make deterministic calculations, despite the great variability associated with fatigue failure.

Regarding the results obtained on the probabilistic prediction of failure shown in this paper, it is important to mention that both approaches (linear and bilinear) have reported different predictions of failure, but the main differences appear for high probabilities of failure, which is not the area of interest. In the lower part of the cdf obtained, associated to lower probabilities of failure, both approaches give similar results, although the linear model seems to be more conservative in all cases. Nevertheless, it is crucial to highlight that it con not confirmed that the Linear Model will be always more conservative than the Bilineal model, because it depends on the material p-S-N field and the stress distribution of the component to be designed.

Note that the model is implemented for different mesh sizes in order to confirm it to be mesh-independent, even though the size of each mesh element is used in the model to obtain the local and global probabilities.

7. Conclusions

The main conclusions to be drawn from the former Sections are the following:

- A probabilistic extension of the linear and bilinear Basquin fatigue models is developed, which enables them to be defined as p-S-N fields.
- An algorithm is provided to define the boundary between the two regions in which a bilinear fatigue model is divided based on the compatibility between the failure distributions on both regions. Contrary to other models, it is automatically determined excluding subjective factors, i.e. user's criteria.
- A methodology for considering the scale effect is presented that ensures transferability of the experimental results from fatigue characterization programs to the design of real components. It allows the local distribution of stress amplitude, or any other generalized parameter, on the scale effect to be considered.

- Based on the proposed enhanced models, a methodology is developed to achieve a probabilistic analysis of damage accumulation. It enables probabilistic failure prediction for components subject to non-constant amplitude loading, in particular random loading, to be performed.
- The models and methodologies presented on this paper are exemplary implemented into a commercial software (NCode) in order to promote their dissemination to the practical structural and component fatigue design.
- A practical example is chosen to illustrate the applicability of the proposed enhanced models and scale effect methodology presented in this paper.

References

[1] W. Cui, "A state-of-the-art review on fatigue life prediction methods for metal structures," *J. Mar. Sci. Technol.*, vol. 7, no. 1, pp. 43–56, 2002, doi: 10.1007/s007730200012.

[2] A. Fatemi and L. Yang, "Cumulative fatigue damage and life prediction theories: A survey of the state of the art for homogeneous materials," *Int. J. Fatigue*, vol. 20, no. 1, pp. 9–34, 1998, doi: 10.1016/S0142-1123(97)00081-9.

[3] SMITH KN, WATSON P, and TOPPER TH, "Stress- strain function for the fatigue of metals," *J Mater*, vol. 5, no. 4, pp. 767–778, 1970.

[4] A. Fatemi and D. F. Socie, "A CRITICAL PLANE APPROACH TO MULTIAXIAL FATIGUE DAMAGE INCLUDING OUT-OF-PHASE LOADING," *Fatigue Fract. Eng. Mater. Struct.*, vol. 11, no. 3, pp. 149–165, 1988, doi: 10.1111/j.1460-2695.1988.tb01169.x.

[5] A. Carpinteri, A. Spagnoli, and S. Vantadori, "A review of multiaxial fatigue criteria for random variable amplitude loads," *Fatigue and Fracture of Engineering Materials and Structures*, vol. 40, no. 7. Blackwell Publishing Ltd, pp. 1007–1036, Jul. 01, 2017, doi: 10.1111/ffe.12619.

[6] O. H. Basquin, "The Exponential Law of Endurance Tests," *Proceedings, Am. Soc. Test. Mater. ASTEA*, vol. 10, pp. 625–630, 1910.

[7] ASTM International, "ASTM E739-10(2015) Standard Practice for Statistical Analysis of Linear or Linearized Stress-Life (S-N) and Strain-Life (ε-) Fatigue Data," *Annual Book of ASTM Standards*, vol. i, no. Reapproved. pp. 1–7, 2015, doi: 10.1520/E0739-10R15.

[8] *VDI 2230 Blatt 1 - 2015-11 - Systematic calculation of highly stressed bolted joints - Joints with one cylindrical bolt*. 2015.

[9] "EN 1993-1-9: Eurocode 3: Design of steel structures - Part 1-9: Fatigue," 2005.

[10] R. Rennert, E. Kullig, M. Vormwald, A. Esderts, and D. Siegele, *Analytical Strength Assesment of Components*. VDMA Verlag, 2012.

[11] A. Hobbacher and International Institute of Welding. Joint Working Group XIII-XV., *Recommendations for fatigue design of welded joints and components : IIW document IIW-2259-I5 ex XIII-2460-13/XV-1440-13*. .

[12] "DNV GL- Guideline for the Certification of Offshore Wind Turbines - ," 2012.

[13] "DNV GL- Guideline for the Certification of Wind Turbines - ," 2010.

[14] J. F. Barbosa, J. A. Correia, R. Freire Júnior, S.-P. Zhu, and A. M. De Jesus, "Probabilistic S-N fields based on statistical distributions applied to metallic and composite materials: State of the art," *Adv. Mech. Eng.*, vol. 11, no. 8, p. 168781401987039, Aug. 2019, doi:

10.1177/1687814019870395.

[15] E. Castillo and A. Fernández-Canteli, *A unified statistical methodology for modeling fatigue damage*. Springer Netherlands, 2009.

[16] V. V. Bolotin, “Wahrscheinlichkeitsmethoden zur Berechnung von Konstruktionen. Berlin, VEB Verlag für Bauwesen ,” vol. 567 S., M 74, no. BN 5615607, 1981, doi: 10.1002/zamm.19830631120.

[17] V. V. Bolotin, *Mechanics of fatigue*. CRC Press, 1999.

[18] A. M. Freudenthal and E. J. Gumbel, “Physical and Statistical Aspects of Fatigue,” *Adv. Appl. Mech.*, vol. 4, no. C, pp. 117–158, Jan. 1956, doi: 10.1016/S0065-2156(08)70372-7.

[19] A. M. Freudenthal, “The statistical aspect of fatigue of materials,” *Proc. R. Soc. London. Ser. A. Math. Phys. Sci.*, vol. 187, no. 1011, pp. 416–429, Dec. 1946, doi: 10.1098/rspa.1946.0086.

[20] M. Muñiz Calvente, “The generalized local model: a methodology for probabilistic assessment of fracture under different failure criteria,” Universidad de Oviedo, Oviedo, 2017.

[21] P. H. Wirsching, “Probabilistic Fatigue Analysis,” in *Probabilistic Structural Mechanics Handbook*, Springer US, 1995, pp. 146–165.

[22] D. S. Paolino, A. Tridello, G. Chiandussi, and M. Rossetto, “Estimation of P-S-N curves in very-high-cycle fatigue: Statistical procedure based on a general crack growth rate model,” *Fatigue Fract. Eng. Mater. Struct.*, vol. 41, no. 4, pp. 718–726, Apr. 2018, doi: 10.1111/ffe.12715.

[23] T. Tomaszewski, P. Strzelecki, A. Mazurkiewicz, and J. Musiał, “Probabilistic Estimation of Fatigue Strength for Axial and Bending Loading in High-Cycle Fatigue,” *Materials (Basel).*, vol. 13, no. 5, p. 1148, Mar. 2020, doi: 10.3390/ma13051148.

[24] P. Strzelecki, “Accuracy of determined S-N curve for constructional steel by selected models,” *Fatigue Fract. Eng. Mater. Struct.*, vol. 43, no. 3, pp. 550–557, Mar. 2020, doi: 10.1111/ffe.13139.

[25] C. Boller and T. Seeger, *Materials data for cyclic loading. Part. B, Low-alloy steels*. .

[26] A. Bernard and E. J. Bos-Levenbach, *The plotting of observations on probability-paper*, no. SP 30a/55. Stichting Mathematisch Centrum, 1955.

[27] J. I. McCool, *Using the Weibull Distribution*. Wiley Series in Probability and Statistics , 2012.

[28] B. Waloddi Weibull, “A Statistical Distribution Function of Wide Applicability,” *J. Appl. Mech*, vol. 18, pp. 293–297, 1951.

[29] J. Gao and Y. Yuan, “Small sample test approach for obtaining *P - S - N* curves based on a unified mathematical model,” *Proc. Inst. Mech. Eng. Part C J. Mech. Eng. Sci.*, p. 095440622092584, May 2020, doi: 10.1177/0954406220925845.

[30] F. W. Scholz and M. A. Stephens, “K-sample Anderson–Darling tests,” *J. Am. Stat. Assoc.*, vol. 82, no. 399, pp. 918–924, 1987, doi: 10.1080/01621459.1987.10478517.

[31] M. Muniz-Calvente, A. M. P. de Jesus, J. A. F. O. Correia, and A. Fernández-Canteli, “A methodology for probabilistic prediction of fatigue crack initiation taking into account the scale effect,” *Eng. Fract. Mech.*, 2017, doi: 10.1016/j.engfracmech.2017.04.014.

[32] A. Carpinteri, A. Spagnoli, and S. Vantadori, “Size effect in S-N curves: A fractal approach to finite-life fatigue strength,” *Int. J. Fatigue*, vol. 31, no. 5, pp. 927–933, May 2009, doi: 10.1016/j.ijfatigue.2008.10.001.

[33] D. S. Paolino, A. Tridello, G. Chiandussi, and M. Rossetto, "On specimen design for size effect evaluation in ultrasonic gigacycle fatigue testing," *Fatigue Fract. Eng. Mater. Struct.*, vol. 37, no. 5, pp. 570–579, May 2014, doi: 10.1111/ffe.12149.

[34] M. A. Miner, "Cumulative damage in fatigue," *J. Appl. Mech.*, vol. 12, p. 159-164, 1945.

[35] M. Muñiz-Calvente, A. Ramos, V. Shlyannikov, M. J. Lamela, and A. Fernández-Canteli, "Hazard maps and global probability as a way to transfer standard fracture results to reliable design of real components," *Eng. Fail. Anal.*, vol. 69, 2016, doi: 10.1016/j.engfailanal.2016.02.004.

[36] S. Blason, J. A. F. O. Correia, A. M. P. De Jesus, R. A. B. Calcada, and A. Fernandez-Canteli, "A probabilistic analysis of Miner's law for different loading conditions," *Struct. Eng. Mech.*, vol. 60, no. 1, pp. 71–90, Oct. 2016, doi: 10.12989/sem.2016.60.1.071.

[37] M. Escalero *et al.*, "Study of alternatives and experimental validation for predictions of hole-edge fatigue crack growth in 42CrMo4 steel," *Eng. Struct.*, vol. 176, pp. 621–631, Dec. 2018, doi: 10.1016/j.engstruct.2018.09.017.

APPENDIX A:

Table A1. Experimental results evaluated

Cycles	Stress (MPa)
248	890,4
260	947,5
280	934,8
300	933,7
750	822,8
770	790,6
1050	793,1
1270	796,6
5000	679,2
7700	665,3
7950	668,8
17200	649,6
18400	637,3
27900	639,5

81000	595,7
90000	595,7
152000	586,4
195000	553,3
290000	558,7